Nuclear Instruments and Methods in Physics Research A 335 (1993) 523–527
North-Holland

NUCLEAR
INSTRUMENTS
& METHODS
IN PHYSICS
RESEARCH
Section A

A neutron diffraction study on the very narrow dynamical width of GaAs [200]

K.-D. Liss and A. Magerl
Institut Laue-Langevin, F-38042 Grenoble Cédex, France

W. Gläser
Technische Universität München, Physikdepartment, D-85748 Garching, Germany

Received 9 June 1993

The energy resolution associated with a particular Bragg reflection is limited by the diffraction properties and by the quality of the material. It can be derived from the structure factor within the dynamic theory of diffraction for ideal crystals. Using the GaAs [200] reflection on a neutron backscattering spectrometer we could realize a resolution of $\Delta E = (43 \pm 5)$ neV. This is an improvement by about a factor of 3 as compared to the value calculated for ideal Si [111] and by about a factor of 7 as compared to the best experimental energy resolution available of any crystal spectrometer.

1. Introduction

The backscattering spectrometer was developed as an extremely successful technique in high resolution neutron spectroscopy [1,2]. In this technique large scattering angles near 180° are used both at the monochromator and the analyzer crystals and the energy resolution is dominated by the uncertainty of the lattice parameter. This value is given by the width of the Darwin curve for ideal crystals. It can be shown, that angular dependencies like the beam divergence or the mosaic spread of the crystal contribute only in second order to the energy resolution. Heidemann and Scholz [1] have demonstrated in a pioneering work the possibility to reach the theoretical resolution for Si [111] of 121 neV in backscattering geometry which corresponds to the convoluted Darwin width of two ideal crystals. This limit is given by the interaction of the neutron wave with the crystal lattice and it is proportional to the structure factor of the Bragg reflection used.

To date there are only two backscattering machines on cold sources available located at the KFA at Jülich and at the ILL, Grenoble [3]. In their normal setup, they employ Si [111] crystals for both monochromator and analyzer. The energy resolution depends on instrumental design parameters and on the crystal quality and it is limited to 300 neV (FWHM). In the present study, we addressed the resolution associated with the GaAs [200] reflection which has a very small structure factor and hence holds promise for a significantly improved energy resolution if the structural quality of the crystals is sufficient [4].

2. Theoretical background

This chapter resumes important results of the dynamical theory of diffraction needed to describe a Bragg reflection in backscattering geometry [5–8].

The reflection profile of the Bragg line is described by Ewald's function

$$\phi(y) = \begin{cases} 1 & |y| \le 1, \\ 1 - \sqrt{\dfrac{y^2 - 1}{|y|}} & |y| > 1, \end{cases} \tag{1}$$

with

$$y = \frac{E - E_0}{E_0} \frac{\pi V_z}{\lambda^2 |F^{\mathrm{b}}_{hkl}|}. \tag{2}$$

E_0 denotes the energy at the center of the Bragg-peak, V_z the volume of the unit cell, λ the wavelength and F^{b}_{hkl} the structure factor including the coherent scattering length. The full width at half maximum of the Ewald function is given by

$$y_{\mathrm{H}} = 4/\sqrt{3}. \tag{3}$$

0168-9002/93/$06.00 © 1993 – Elsevier Science Publishers B.V. All rights reserved

Table 1
Comparison between theoretical and experimental values of various properties of the transmission profiles for Si [111] and GaAs [200] reflections

Quantity	Formula sign	Theory Si [111]	IN10 Si [111]	Theory GaAs [200]	Experiment GaAs [200]
Absolute convoluted line width	ΔE	121 neV	300 neV	13.0 neV	43 ± 5 neV
Relative Line width	$\Delta E/E$	58.3×10^{-6}	144×10^{-6}	5.07×10^{-6}	$(17 \pm 2)\times10^{-6}$
Integrated reflectivity	R_E	120 neV	120 neV	12.8 neV	33 ± 5 neV
Line depth	τ	0.7262	0.2	0.7262	0.49 ± 0.05

With eqs. (2) and (3) the relative energy width is

$$\frac{\Delta E_H}{E_0} = \frac{4}{\sqrt{3}} \frac{\lambda^2 |F^b_{hkl}|}{\pi V_z}. \tag{4}$$

The integrated reflectivity R_y in dimensionless units is given by

$$R_y = \pi \tag{5}$$

or on the energy scale

$$R_E = R_y \frac{\Delta E_H}{y_H} = \frac{\sqrt{3}}{4} \pi \Delta E_H. \tag{6}$$

The above quantities correspond to the reflection on only one crystal. The convolution of two identical Ewald functions appropriate for a double crystal diffractometer [1] enlarges these quantities by a factor

$$f = \pi/(2\pi - 4) \approx 1.1376 \quad \text{or} \quad \Delta E/E_0 = f \Delta E_H/E_0. \tag{7}$$

However, the peak reflectivity $\tau_H = 1$ for a Bragg reflection is reduced for the convoluted line by f to

$$\tau = 1/f. \tag{8}$$

The theoretical values in table 1 are evaluated from these formulae.

3. Instrumental setup

A dedicated test bench in transmission-reflection geometry has been set up to measure the GaAs [200] reflection. Besides of the detector there were no further elements between the two crystals (fig. 1). The incident beam from the cold source is pre-monochromized by a graphite crystal deflector and a polycrystalline beryllium filter. This beam still contains a large energy distribution of $\Delta E/E \approx 0.01$ centered around $E_0 = 2.56$ meV. Because this energy width covers the whole scanning range of the subsequent instrument, it is referenced further as a white beam. A 50% chopper triggers a semitransparent detector. The monochromator crystal K_1 is mounted on a goniometer table and the analyzer K_2 is attached to the Doppler drive. A neutron package originating at the chopper meets the monochromator crystal K_1 where a well defined energy E_1 is diffracted out of the white beam. The remainder of the neutron package travels through the semitransparent detector and meets the analyzer K_2 which reflects a well defined energy E_2 back towards the detector. The detector electronics is gated such, that only neutrons traveling back from K_2 are counted. The analyzer energy E_2 is scanned by a Doppler motion of K_2. The neutron intensity plotted against E_2 will show a minimum for $E_1 = E_2$.

4. Crystal alignment

Great care is needed to align both crystals parallel to each other. First the crystal K_2 is adjusted without the monochromator in position. The full width at half maximum $\Delta\Phi$ of the reflection curve as a function of the rocking angle is given by the ratio of the size of the detector b with the distance A between analyzer K_2 and detector D:

$$\Delta\Phi = b/2A. \tag{9}$$

With $b = 2.1$ cm and $A = 72$ cm the calculated value of $\Delta\Phi = 0.84°$ corresponds well with the measured value of $\Delta\Phi \approx 0.7°$ (fig. 2). The monochromator K_1 needs to

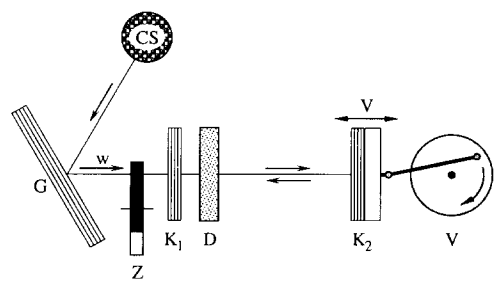

Fig. 1. Instrumental setup. The white neutron beam W coming from the cold source CS and deflected on a polygraphite crystal G is incident to the backscattering bench. The latter consists of the monochromator K_1, the semitransparent detector D and the analyzer K_2 mounted on the Doppler drive V. A chopper Z produces neutron packages and triggers the detector to distinguish the neutrons traveling forward and backward.

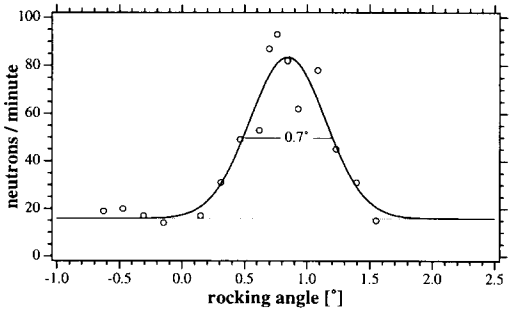

Fig. 2. Rocking curve used for the line up of the analyzer crystal K_2. The width of the rocking curve can be derived from a simple geometric consideration.

be lined up parallel to K_2, already set to its optimum value. The intensity plotted against the tilt or rotation angle of K_1 gives a narrow minimum for the parallel position, because K_1 and K_2 have the same lattice parameter. The width of this minimum can be derived from a Taylor expansion to second order of Bragg's law in $\Delta\Theta$ near the backscattering position of $\Theta = \pi/2$:

$$\lambda = 2d\left(1 - (\Delta\Theta)^2/2\right). \tag{10}$$

From $\Delta\lambda = 2d - \lambda$ follows

$$\Delta\lambda/\lambda = (\Delta\Theta)^2/2 \quad \text{or} \quad \Delta E/E = (\Delta\Theta)^2. \tag{11}$$

The energy resolution $\Delta E/E$ is given by eq. (4), and

$$\Delta\Theta = \sqrt{\Delta E/E} \tag{12}$$

is obtained. Using the structural properties of GaAs [200] and for backscattering geometry we obtain $\Delta E/E = 3.7 \times 10^{-6}$ and $\Delta\Theta = 0.11°$. The measured curve plotted in fig. 3 reveals $\Delta\Theta \approx 0.12°$. This agreement confirms the parallel alignment of crystals K_1 and K_2.

5. Experimental results

In fig. 4 a typical neutron spectrum is plotted as a function of the neutron energy. The intensity has been

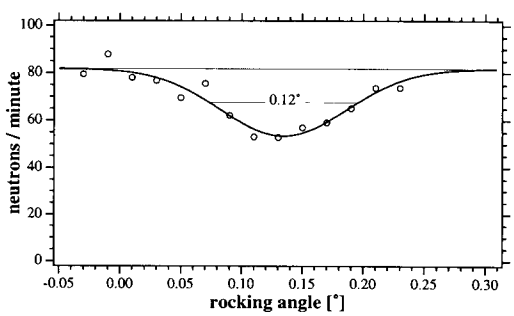

Fig. 3. Rocking curve of the monochromator K_1.

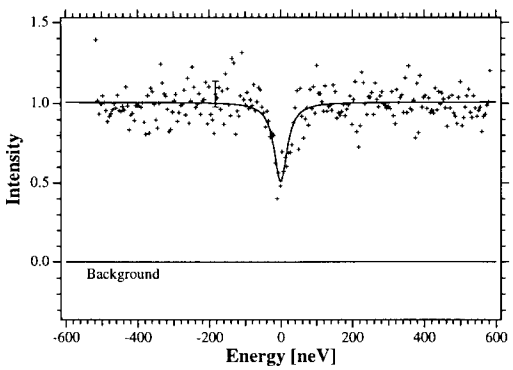

Fig. 4. Measured Bragg line of the GaAs [200] reflection. The spectrum is normalized to the incident white beam by a monitor. The width of the fitted Lorentz line is 43 neV. A typical error bar is plotted to the left of the minimum.

normalized to the incident white beam by a reference scan with the monochromator K_1 removed. In addition a background measured by taking off the analyzer K_2 has been subtracted from the data. A total of 62653 neutrons were counted in the entire energy range during the measuring time of 14 h. The Bragg line shows a width of $\Delta E = 43 \pm 5$ neV. The integrated reflectivity represented by the intensity removed from the white spectrum is $R_E = 33 \pm 5$ neV with a depth of $\tau = 0.49 \pm 0.05$. Measured and theoretical values for GaAs [200] are listed in table 1 and compared with the values for Si [111].

6. Discussion

As the salient feature of the present study we note that the experimental energy resolution $\Delta E = 43$ neV for GaAs [200] is seven times smaller than the best energy resolution of a today's backscattering spectrometer set up with perfect Si [111] crystals (≈ 300 neV). This value is also three times smaller than the natural line width of Si [111]. This opens up the possibility for a new generation of ultra high resolution crystal spectrometers in condensed matter science.

Still, the experimental values given in table 1 differ from the theoretical results. The measured line is about a factor 3.3 larger and its integrated reflectivity is 2.6 times higher than predicted. At the same time the depth of the reflection profile is reduced by a factor of 0.67.

The last point could be explained by fluctuations of the Bragg peak position caused for example by temperature instabilities or mechanical vibrations. This would increase the width and decrease the depth of the line. Note, however, that the integrated intensity would not change in this case. Quantitatively, the line broadening

between the observed and the theoretical values amounts to

$$\varepsilon/E_0 = 12 \times 10^{-6}. \tag{13}$$

This can originate from several mechanisms which will be discussed in the following:

6.1. Temperature fluctuations

The temperatures of the two crystals are not identical during the time of the measurement. A difference of ΔT induces a line broadening of

$$\left.\frac{\varepsilon}{E_0}\right|_T = 2\alpha(T)\Delta T, \tag{14}$$

with a thermal expansion coefficient is $\alpha(300\ \mathrm{K}) = 5.7 \times 10^{-6}$ for GaAs. Thus a temperature difference of

$$\Delta T = 1\ \mathrm{K} \tag{15}$$

suffices to account for the observed broadening.

6.2. Vibrations

Mechanical vibrations e.g. created by the motor of the Doppler drive with velocity V broaden the line width by

$$\left.\frac{\varepsilon}{E_0}\right|_V = 2\frac{V}{v_0}. \tag{16}$$

The neutron velocity is $v_0 = 7.0 \times 10^5$ mm/s. Vibrations provoking non-controlled motions with

$$V = 4\mathrm{mm/s} \tag{17}$$

would account for the observed broadening.

6.3. Crystal distortions

Macroscopic bending of the crystal or microscopic lattice defects may give rise to a strained lattice yielding distortions $\Delta L/L$ of the lattice spacing. This broadens the transmission spectrum by

$$\left.\frac{\epsilon}{E_0}\right|_S = \left\langle\frac{\Delta L}{L}\right\rangle. \tag{18}$$

The bracket $\langle\ \rangle$ stands for an average over all distortions. A value of

$$\left\langle\frac{\Delta L}{L}\right\rangle = 6 \times 10^{-6} \tag{19}$$

is sufficient for the experimental line broadening.

6.4. Misorientation

A misorientation of the crystal planes in K_1 and K_2 by an angle β results in a line broadening by

$$\left.\frac{\epsilon}{E_0}\right|_\beta = 2\beta\delta, \tag{20}$$

where δ is the angular divergence of the neutron beam. In our case $\delta = 2°$, and a value of

$$\beta = 35'' \tag{21}$$

would be required to explain the observed line width.

7. Error sources

In the previous section we mentioned possible mechanisms for the observed line broadening. All possibilities mentioned may contribute very sensitively as can be seen by the considerations given above.

– The temperature was not controlled during the experiment. Although a box between the chopper and the Doppler drive was installed, air flows at the crystals were not completely eliminated. We can estimate from the conditions in the laboratory that these temperature fluctuations do not play the main role in the line broadening, but this effect has to be investigated for a future set up.

– Vibrations from the Doppler drive are hard to control. The velocity pick-up is made from a permanent magnet moving in an induction coil. The magnet is mounted directly to the support of the moving crystal K_2. The Doppler device designed for the Si [111] resolution may still have residual vibrations mainly induced by the driving motor. These vibrations can influence the measurement in two ways: First, high frequency vibrations with a time period shorter than the traveling time of the neutron through the detector are not resolved. Second, mechanical resonance vibrations can result in an unknown phase shift between the real crystal velocity and the pick-up magnet giving a wrong signal to the multi-channel-analyzer.

– Intrinsic strain of the crystals is created during crystal growth and cannot be excluded. According to the producer, the crystals have a quite important dislocation density of about

$$\rho = 2.6 \times 10^3\ cm^{-2}. \tag{22}$$

This mechanism does not only broaden the line but it also increases the integrated reflectivity.

– Similar effects result from macroscopic stress on the crystals, for example by bending them in the crystal holders.

– A misalignment of the crystals plays a very sensitive role to the line broadening related to the high beam divergence. Fig. 3 shows a spectrum taken during the adjustment of K_1 and K_2. The crystals must be aligned parallel to better than $\frac{1}{2}$ min of arc which means that they have to be adjusted to $\frac{1}{15}$ to the width of the curve given in the figure to obtain the measured line width. Dislocation walls and other lattice faults may contribute to intrinsic inclinations and have the same effect than the error in adjustment.

8. Conclusion

The present investigation has demonstrated the potential to build higher resolution backscattering spectrometers than those equipped with Si [111]. The measured Bragg line of GaAs [200] with $\Delta E = (43 \pm 5)$ neV is about 3 times narrower than the theoretical predicted Darwin width of Si [111]. Compared with the today's resolution on backscattering spectrometers, the improved value is 7 times higher. However, the theoretical possible value of $\Delta E = 13.0$ neV for GaAs [200] has not been achieved.

A backscattering spectrometer with a largely improved energy resolution, a dynamical range of -15 μeV $< \Delta E < 15$ μeV like on existing machines and with a range of momentum transfer of $Q < 2.2$ Å^{-1} would open a new order of magnitude in inelastic spectroscopy. We want to highlight only two examples where we feel that an improved energy resolution will allow to explore new fields in science.

– The level scheme of tunneling motions of hydrogenous molecular crystals as studied on various compounds by neutron spectroscopy is a very sensitive probe for the molecular environment. The energy transfer for the deuterated species are largely reduced due to the increased mass of the tunneling entity and they have been measured only for a few exceptional systems. Even in these rare cases it is extremely difficult to obtain information about a possible intrinsic line broadening of the excitations due to insufficient instrumental energy resolution. E.g. there is no tunneling data on the effect of a statistically disturbed environment of a deuterated molecular unit as realized in a dilution experiment which could than be compared with existing data for the hydrogenated molecule.

– Even at the melting point the diffusion constant for metals rarely exceeds 10^{-8} cm^2/s which means that it is not accessible by high resolution quasi-elastic neutron scattering. There exist only a few examples all based on a bcc structure like the self diffusion of Na close to the melting point [9] or the anomalous fast diffusion of β-Ti [10] where neutron scattering could be used. An improvement of the energy resolution as mentioned above would largely extend the number of metallic systems accessible to quasi-elastic neutron scattering including even fcc-based materials (a sufficiently high neutron flux can be provided by including focusing components whenever appropriate).

Although this work has been done on the GaAs [200] reflection, any crystal of good quality having a reflection with a smaller structure factor than Si [111] is suitable for a higher resolution backscattering set up. Of course there should be no other inconveniences like absorption or activation of the material. However, the activities on GaAs crystals relating to the semiconductor industry push the present development for large crystals with good and homogeneous lattice properties in the near future.

Acknowledgement

We thank Dr. H. Rüfer, Wacker Chemitronic GmbH, Burghausen, Germany and Dr. K. Sassa, Mitsubishi Metal Corporation, Saitama, Japan who provided GaAs crystals for the present study.

References

[1] A. Heidemann and J. Scholz, Z. Physik 263 (1973) 291.
[2] M. Birr, A. Heidemann and B. Alefeld, Nucl. Instr. and Meth. 95 (1971) 435.
[3] H. Blank and B. Maier, Guide to Neutron Research Facilities at the ILL, Institute Laue-Langevin Grenoble, France (1988).
[4] B. Alefeld and T. Springer, Nucl. Instr. and Meth. A 295 (1990) 268.
[5] C.G. Darwin, Philos, Mag. 27 (1914) 315; and 27 (1914) 657.
[6] P.P. Ewald, Ann. Physik 54 (1917) 519.
[7] H. Rauch and D. Petrascheck: Grundlagen für ein Laue-Neutroneninterferometer Teil I: Dynamische Beugung, Atominstitut der Österreichischen Universitäten (1976).
[8] H. Rauch, D. Petrascheck, in: Neutron Diffraction, ed. H. Dachs (Springer, Berlin, Heidelberg, New York, 1978) p. 303.
[9] G. Göltz, A. Heidemann, H. Mehner, A. Seeger and D. Wolf, Phil. Mag. 41 (1980) 723.
[10] G. Vogl, W. Petry, Th. Flottmann and A. Heiming, Phys. Rev. B39 (1989) 5025.